

CBCT Validation Study on Intraclass Correlation for Linear Measurements in Peri-implantitis: an Observational Study

Amanda Beatriz Rodriguez¹, Berceste Guler Ayyildiz^{1,2}, Halil Ayyildiz^{1,3}, Aniruddh Narvekar¹, Mohammed H. Elnagar⁴, Michael Schmerman¹, Grace Viana⁴, Salvador Nares¹, Tolga Fikret Tözüm¹

¹Department of Periodontics, College of Dentistry, University of Illinois Chicago, 60612, Chicago, USA.

²Department of Periodontology, Faculty of Dentistry, Kütahya Health Sciences University, 43100, Kütahya, Türkiye.

³Department of Oral and Maxillofacial Radiology, Faculty of Dentistry, Kutahya Health Science University, 43100, Kütahya, Türkiye.

⁴Department of Orthodontics, College of Dentistry, University of Illinois Chicago, 60612, Chicago, USA.

Corresponding Author:

Amanda B. Rodriguez

Department of Periodontics, College of Dentistry

University of Illinois Chicago

801 S Paulina St, Room 330D, 60612 Chicago, Illinois

USA

Phone: +1-786-961-7953

E-mail: arodr368@uic.edu

ABSTRACT

Objectives: This retrospective observational study aimed to evaluate the reliability and reproducibility of intra-examiner and inter-examiner bone loss measurements in cone-beam computed tomography images over time, on patients with peri-implant defects using two cone-beam computed tomography software programs: 3D Slicer and Dolphin Imaging.

Material and Methods: Baseline images were oriented based on implant location and aligned with the palatal or Go-Me plane. Two CBCT volumes were imported and superimposed using landmark-based and surface-based methods, with accuracy assessed through 3D and 2D matching. Measurements of implant diameter, length, and bone thickness at 0, 1, 3, and 5 mm intervals were taken at two-time points by three independent examiners, with reliability assessed using intra-class correlation coefficients.

Results: Twenty measurements per 14 cases were evaluated. Each examiner conducted 1,120 measurements with a cumulative total of 3,360 measurements assessed. Significant differences in measurement times were observed, with 3D Slicer requiring more time for superimposition tasks ($P < 0.001$). Both software programs, however, demonstrated high reliability (intraclass correlation coefficient > 0.80) in inter- and intra-examiner agreement across various bone measurements.

Conclusions: Findings emphasize that the high reliability observed with the software and superimposition techniques is directly linked to the calibration and training exercises conducted with the examiners before the study. Dolphin's Imaging automated superimposition was significantly faster than 3D Slicer's manual approach, 3D Slicer offered superior image quality and better differentiation of bone outlines. Both software demonstrated effectiveness in delivering consistent and reproducible measurements, with significant implications for clinical and research applications in implant dentistry.

Keywords: tomography; calibration; anatomy; bone; peri-implantitis.

Accepted for publication: 31 March 2025

To cite this article:

Rodriguez AB, Ayyildiz BG, Ayyildiz H, Narvekar A, Elnagar MH, Schmerman M, Viana G, Nares S, Tözüm TF.

CBCT Validation Study on Intraclass Correlation for Linear Measurements in Peri-implantitis: an Observational Study
J Oral Maxillofac Res 2025;16(1):e4

URL: <http://www.ejomr.org/JOMR/archives/2025/1/e4/v16n1e4.pdf>

doi: [10.5037/jomr.2025.16104](https://doi.org/10.5037/jomr.2025.16104)

INTRODUCTION

Dental implants are considered the treatment of choice to replace missing teeth in single, partially, and fully edentulous patients with high survival rates and predictable long-term outcomes [1]. Peri-implantitis is a multifactorial condition characterized by inflammation of peri-implant soft tissue, resulting in irreversible bone loss [2]. Peri-implant mucositis has a prevalence of 43% [3], and peri-implantitis affects 22% of cases, with a range from 1% to 47% [4-6].

Diagnostic tools currently used in dentistry are clinical examination (percussion, palpation, visual inspection), intraoral photography, periodontal probing, two-dimensional (2D) radiographs (panoramic, intraoral X-rays), and three-dimensional (3D) imaging techniques such as cone-beam computed tomography (CBCT) and intraoral (IO) scans [7]. The use of diagnostic tools provides a better understanding of the anatomy, pathologies, and lesions of the oral cavity [7,8].

To date, numerous studies have demonstrated the importance of radiographic imaging modalities for the diagnosis of bone defects [9]. Clinical examination of peri-implant and periodontal tissues assesses soft tissue inflammation and hard tissue destruction but has limitations due to variability in measurements like probing depth (PD), bleeding on probing (BOP), and clinical attachment level (CAL). These measurements can be affected by factors such as tissue access, crown overcontouring, interdental spaces, and probing force and angle [7,10]. 2D radiographs, though widely used, only provide a projection of the maxilla and mandible's 3D structure [7]. They measure interproximal bone levels and the extent of bone loss but have limitations like superimposition, underestimation of disease, distortion, and blurring, which can affect diagnostic accuracy [7].

CBCT, provides detailed cross-sectional images, reconstructed into 3D models for assessing bone morphology, anatomical variations, and vital structures [7,10,11]. However, CBCT has disadvantages like radiation exposure, cost, low soft tissue contrast, and artifacts from metallic objects [12]. The use of CBCT as a well-established diagnostic tool for treatment planning and digital simulation for implant placement is well documented [13,14]. For clinical applications, CBCT is highly accurate and provides reliable linear measurements [13-15]. Previous pre-clinical studies have evaluated CBCT accuracy measurements in cadavers [16,17], and *in vivo* [18-20]. Moreover, the correlation between CBCT and reference standards was evaluated

[15,19,21], and agreement was evaluated [15,22]. The results of several authors showed a high correlation between the CBCT and gold standards using different parameters [19,21].

In various CBCT studies [13,23], the reliability of intra-examiner and inter-examiner correlations has been demonstrated, supported by advanced software facilitating accurate measurements among different professionals. To the best of our knowledge, this is the first study to compare the use of two CBCT software programs for peri-implant hard tissue evaluation in dentistry. Specifically, 3D Slicer software version 5.3.1 (The 3D Slicer Community; Texas, USA - www.slicer.org), an open-source software widely used for engineering and biomedical data analysis [24], and Dolphin Imaging version 11.5 Premium (Patterson Dental Supply, Inc. dba Dolphin Imaging and Management Solutions, Chatsworth, CA, USA - www.dolphinimaging.com), which is commonly employed in dentistry for orthodontic assessment, including skeletal growth and tooth movement evaluation [25]. Therefore, this retrospective observational study aims to evaluate the reliability and reproducibility of intra-examiner and inter-examiner bone loss (linear) measurements with superimposing cone-beam computed tomography images longitudinally, focusing on patients with peri-implant defects using two cone-beam computed tomography software: 3D Slicer and Dolphin Imaging.

MATERIAL AND METHODS

Study design

Data collection for this retrospective, descriptive, observational study was conducted following the Declaration of Helsinki, and the protocol was approved by the Office for the Protection of Research Subjects (OPRS) of the College of Dentistry (COD) of the University of Illinois Chicago (UIC) on November 22, 2022, for exemption from Institutional Review Board (IRB) with IRB ID (STUDY2022-1465). A total of 14 CBCT scans performed over 20 years (from May 1st 2001 to May 1st 2021) were provided by the University of Illinois Chicago (COD) following the requirements listed in the Investigator Manual (HRP-103) of the IRB system. Additionally, the Strengthening the Reporting of Observational Studies in Epidemiology (STROBE) guidelines were followed. The STROBE flowchart was used to ensure methodological rigor and transparent reporting. A total of 30 CBCT scans were initially assessed for eligibility. Of these, 16 were excluded due to the following reasons: inadequate field of view (FOV)

(n = 1), follow-up time of less than 1 year (n = 12), and missing CBCT data (n = 3). Consequently, 14 studies met the inclusion criteria, were analyzed, and followed up as per the study protocol (Figure 1).

Inclusion criteria

The inclusion criteria were CBCT scans of subjects between the ages of 18 and 70 years, systemically healthy according to the American Society of Anesthesiologists (ASA) I or II and may be either smokers or non-smokers. They must have had at least one dental implant placed at UIC COD with a follow-up period of at least 1 year. Additionally, they must have undergone CBCT imaging before implant placement (BL), and at least one year following implant placement functional loading (T1).

Exclusion criteria

Subjects were excluded if they presented uncontrolled systemic disorders such as osteoporosis, vitamin D deficiency, osteonecrosis of the mandible, cancer, or immunosuppression that may affect bone metabolism are excluded. Those who have undergone orthodontic treatment, take medications known to affect bone

homeostasis (e.g., intravenous or intramuscular bisphosphonates), or lack a baseline (BL) CBCT are also excluded.

Data extraction

A keyword search of COD axiUm® version 2024.2 (Exan Corporation; Vancouver, British Columbia, Canada) database was performed to identify treatment entries for dental implant complications including peri-implantitis, peri-mucositis, implant loss, implant failure, implant bone loss, implant gingival recession, implant inflammation, etc. Demographic data relevant to dental implant therapy such as age at the time of implant placement, sex, ASA classification, tooth number, and type of implant, were included in the study.

CBCT analysis

An i-CAT™ FLX V17 3D CBCT machine (Imaging Sciences International LLC, Hatfield, Philadelphia, USA) with a 0.3 mm voxel size, 120 kV, and 5.0 mA exposure was used to acquire images. The field of view was fixed at 16 cm deep x 6 cm height for the maxilla or mandible, and 16 cm deep x 10 cm height

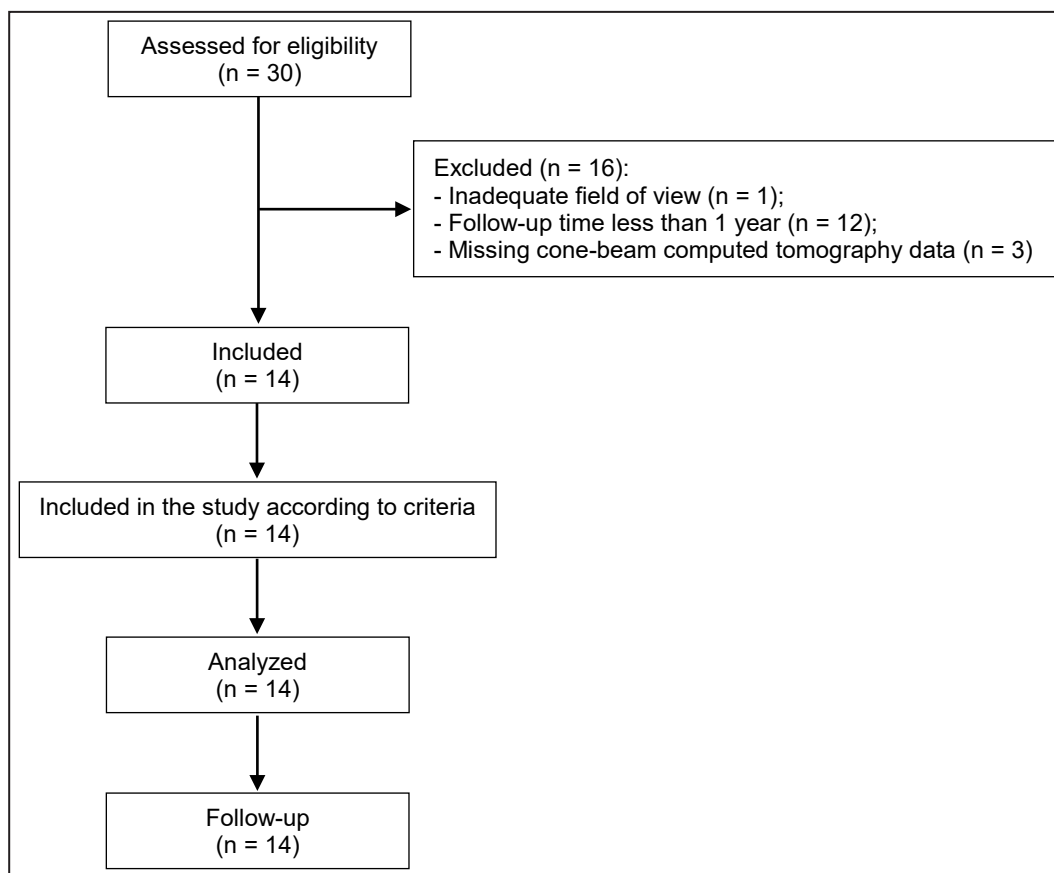


Figure 1. STROBE flowchart. Initially, 30 cone-beam computed tomography scans were assessed for eligibility. As a result, 14 studies met the inclusion criteria and were analyzed.

for both jaws, allowing observation of all relevant anatomical structures. The data was captured in the universal Digital Imaging and Communication in Medicine (DICOM) format (www.dicomstandard.org/) format and displayed in 2D with 3D details. Images were obtained from 200 to 360 slices, converted into DICOM format, and rendered into volumetric images. Sagittal, axial, and coronal slices, as well as 3D reconstructions, were used to determine landmark positions. Baseline CBCT scans were taken before implant placement, with follow-ups based on data examination. Two software programs, 3D Slicer and Dolphin Imaging, were used for analysis. Primary reconstructions were made using the large window setting in the axial slices, oriented to the palatal plane (maxilla) or Go-Me plane (mandible). A total of 14 implants from 14 cases were evaluated by three researchers (A.B.R., B.G.A. and H.A.), with two periodontists and one oral and maxillofacial radiologist. Evaluations were done at two time points in the two softwares, on consecutive days, to reduce operator bias and memory effects while adhering to a consistent workflow.

CBCT measurements

Measurements were conducted at each time point based on standardized criteria, including implant diameter and length, as well as buccal bone thickness at distances of 0, 1, 3, and 5 mm from the implant shoulder. Palatal/lingual bone thickness was assessed at the same intervals in a sagittal view (Figure 2). For all dimensions, the measuring tools were positioned from the external border of each landmark. Implant length was measured from the implant-abutment connection to the most apical

part of the implant. Each examiner identified the landmarks twice in two software programs using 2D images on separate days, with a one-week interval between sessions. A calibration session was conducted where one examiner (A.B.R.), trained the examiners on 3D Slicer, while an experienced orthodontist (E.M.), provided training on Dolphin Imaging. All measurement annotations were blinded to each examiner and between different software platforms to minimize bias and avoid memory recall. Additionally, the time taken for each case evaluation at each time point and with each software was recorded for further analysis (Figure 2). Images were viewed on a Dell HDR screen (Dell Technologies; Texas, USA) with a 2560 x 1440 pixels resolution, 60 Hz, 24-bit, under dimly lit conditions.

3D Slicer workflow

Open-source software 3D Slicer was used for visualization, segmentation, registration, and analysis of DICOM files (536 x 536 x 392 mm³, 0.3 x 0.3 x 0.3 mm spacing) [24]. Baseline (BL) images were oriented depending on the implant location to the palatal or Go-Me plane, and volume rendering was performed with colors assigned for consistency (white for BL, yellow for T1). A second volume was imported and transformed using the same workflow. Superimposition of the two volumes (BL and T1) was done by manual approximation, and then finer superimposing details were achieved by landmark-based and surface-based methods. This was done by using image matching in 3D and later on in 2D in the axial, coronal, and sagittal planes until matching was deemed acceptable by each examiner. Each used the luminosity bar to a 50% to evaluate the accuracy

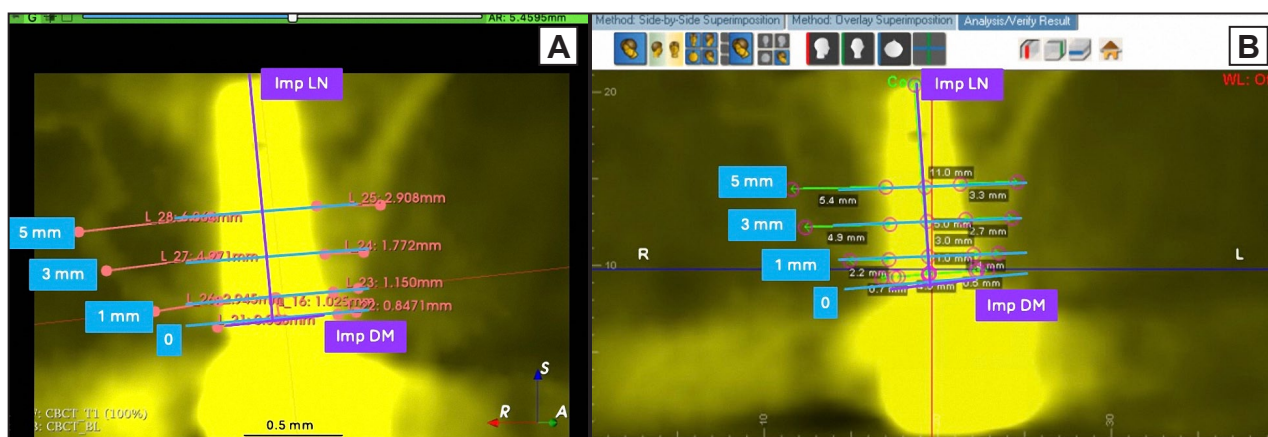


Figure 2. Cone-beam computed tomography measurements. Measurements were illustrated for time point T1 for case 5 (Implant #14) on 3D Slicer (panel A), and Dolphin Imaging (panel B). Blue lines mark the landmarks at the implant shoulder (0), at 1 (1 mm), 3 (3 mm), and 5 mm (5 mm) apical to the implant shoulder for measurement of bone thickness at both buccal and palatal of implant #14 in a cross-sectional view at the mid-sagittal implant slice plane. Additionally, measurements in purple were annotated for implant diameter (Imp DM), and implant length (Imp LN).

of super-imposition. Once the superimposition had taken place, sagittal views of the implant were used to annotate the same cut-plane for respective measurements. After superimposition, sagittal views were used to annotate measurements, and distances between landmarks were automatically calculated. Measurements were performed with the 2D measurement tool, and transparency was set to 50% for evaluating implant differences at each time point (Figure 3).

Dolphin Imaging workflow

The panoramic tool was applied to an axial slice to reconstruct the CBCT data into a panoramic image. The panoramic path was adjusted to ensure all relevant anatomical points were visible. Orientation was set by aligning the volume with the implant location relative to the palatal or Go-Me plane. The volume was rotated to create a reference point, saved as orientation 0. For superimposition, BL was used as the first volume (white) and T1 as the second (yellow). Next, the superimposition was performed using the Overlay Superimposition method by utilizing Voxel-based superimpositions feature setting a cube in the area of interest (maxilla or mandible). Finer details of the superimpositions were achieved by using an automated sub-region marking for auto-superimposition. The digitize/measurement feature was used for annotations, using the “Dolphin” and “2D Line” tools for measurements, and transparency

was set to 100% to assess implants at the same cut-plane. Distances between landmarks were automatically calculated for vertical and horizontal lines (Figure 4).

Statistical analysis

A small sample size of 14 CBCT scans was used since this is a validation study. Each of the 14 cases included 10 measurements, resulting in a total of 560 measurements, which was deemed feasible and supported by a power calculation exceeding 85%. All measurements were made to determine the reproducibility and reliability of the variables measured using the two different software. Intra-examiner and inter-examiner reliability and reproducibility were assessed using the intraclass correlation coefficient (ICC), which ranges from 0 to 1. Higher values indicated greater reliability. An ICC above 0.75 is considered good [26]. The agreement between examiners for 3D Slicer and Dolphin Imaging measurements was evaluated using ICCs with 95% confidence intervals (CI). The analysis was conducted in Statistical Package for Social Sciences (SPSS) version 29.0 (IBM, SPSS Inc., Chicago, IL, USA) to assess intra-rater reliability (agreement between repeated measurements by the examiner) and inter-rater reliability (agreement between measurements by different examiners). A two-way random effects model with absolute agreement in SPSS version 13 by an experienced statistician was used. To interpret

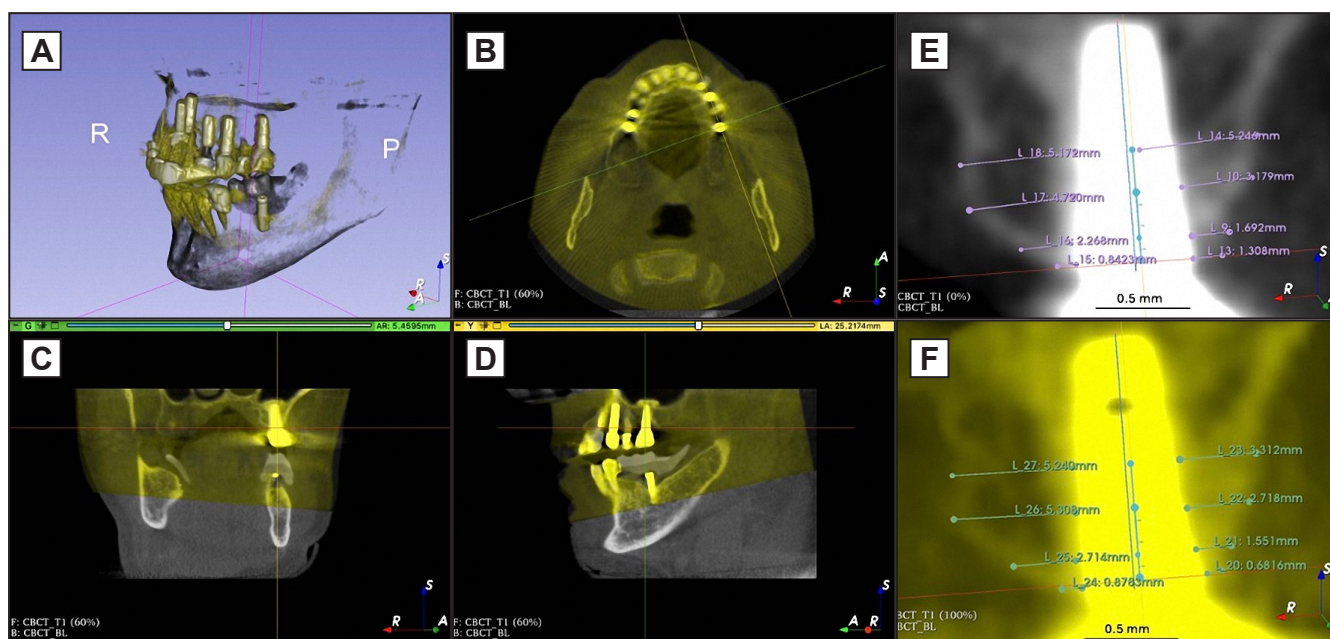


Figure 3. 3D Slicer superimposition workflow. The initial superimposition of the two volumes, BL (white) and T1 (yellow), was achieved through manual approximation (plane A). Finer alignment was followed by adjustments in the 2D axial (plane B), sagittal (plane C), and coronal (plane D) views until an acceptable match was reached. Sagittal views of the implant were used in identical cut-planes for measurements in BL (plane E) and T1 (plane F).

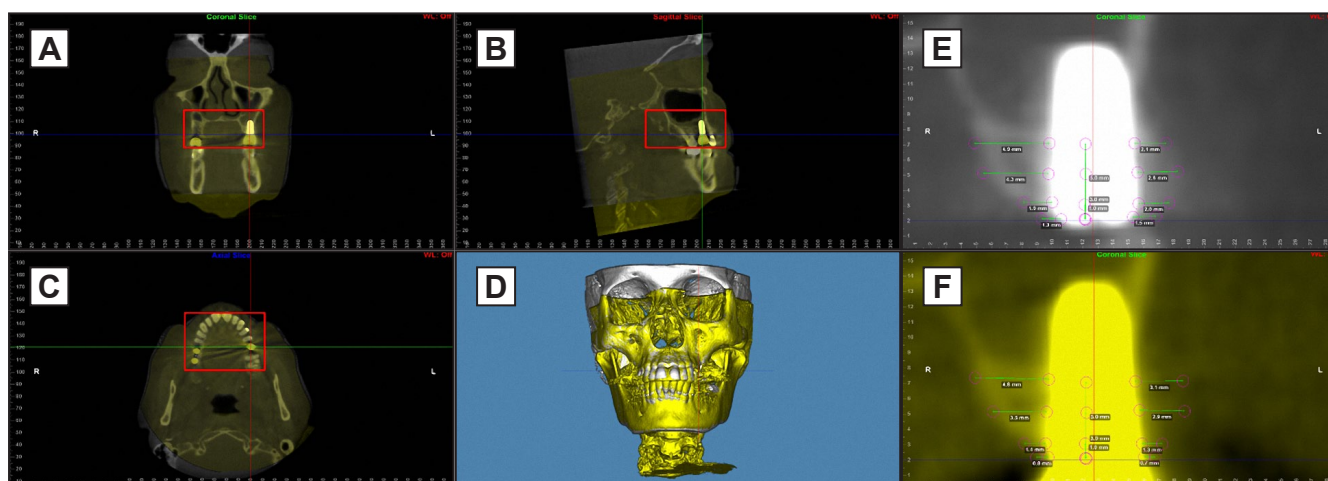


Figure 4. Dolphin Imaging superimposition workflow.

BL was used as the first volume, displayed in white, with T1 added as the second volume, displayed in yellow (planes A, B, C). The superimposition was performed using Voxel-based superimposition feature with a red cube set in the area of interest (maxilla in planes A, B, C). Finer alignment was achieved by marking a sub-region for auto-superimposition (plane D). Annotations were made using the digitize/measurement feature. The distance between landmarks was automatically calculated and displayed as vertical and horizontal 2D lines for BL (plane E) and T1 (plane F).

landmark identification errors, average mean differences between two examiners were summarized, and the coefficient of variation (CV) in % was used to evaluate precision. Inter-examiner variation was tested with paired t-tests, while data distribution was assessed using the Kolmogorov-Smirnov test to choose appropriate statistical methods. Intra-examiner variation was also evaluated with paired t-tests for repeated measurements, and significance was set at $\alpha = 0.01$ to adjust for multiple comparisons.

RESULTS

The patients' ages ranged from 18 to 70 years, with a mean of 62.14 (SD 7.52) years and a median of 66 years. The cohort included 9 females (64.28%) and 4 males. Demographics showed 14.29% had diabetes, 21.43% osteoporosis, and 50% hypertension. Other systemic conditions were present in < 5% of cases. Smoking history: 21.42% current smokers, 28.57% former smokers (average quitting duration 18.6 years), and 50% never smokers. Follow-up duration ranged from 12 to 85 months, with a mean of 42 (SD 23) months. Implants varied in diameter (3.3 to 5 mm) and length (8 to 13 mm), with 7 placed in the maxilla and 7 in the mandible. Implant brands included Astra Tech AB (Mölnådal, Sweden) (7), Osseotite® implant (Biomet; Palm Beach, Florida, USA) (1), from Nobel Biocare AB (Gothenburg, Sweden) (3), and Straumann AG (Basel, Switzerland) (4).

A total of 20 measurements were analyzed for each of the 14 cases, yielding 280 measurements per case. Each examiner evaluated each case twice using

two different software programs, resulting in 1,120 measurements per examiner and 3,360 cumulative measurements across the study. The time for each task (superimposition and measurements) was recorded in minutes and seconds. The longest superimposition (SIP) times were 13 min 60 sec (SD 2 min 30 sec) for 3D Slicer and 6 min 25 sec (SD 1 min 22 sec) for Dolphin Imaging. The shortest SIP times were 10 min 3 sec (SD 2 min 48 sec) for 3D Slicer and 4 min 15 sec (SD 1 min 2 sec) for Dolphin Imaging. For measurements, the longest time was 12 min 25 sec (SD 2 min 58 sec) for 3D Slicer and 8 min 33 sec (SD 3 min 15 sec) for Dolphin Imaging. The shortest measurement times were 6 min 49 sec (SD 1 min 50 sec) for 3D Slicer and 6 min 25 sec (SD 1 min 34 sec) for Dolphin Imaging. Analysis showed significant differences ($P < 0.05$) between 3D Slicer and Dolphin Imaging for SIP times, but no significant differences in measurement times ($P > 0.05$). Significant differences were observed in SIP and measurement times across the three examiners when comparing the two software programs ($P < 0.05$) (Table 1).

The results of this study showed that the ICC for intra- and inter-examiner readings across different methods indicated good agreement, $ICC > 0.8$ (Tables 2 and 3). Regarding intra-examiner analysis, the three examiners showed excellent agreement ($ICC = 0.956$) with repeated measurements at different time points and within different software. This highlights the importance of calibration exercises, landmark delineation, and software training before clinical application and/or research purposes. Additionally, time was recorded between examiners, showing no significant differences in time-performing

Table 1. Average mean times for each examiner and software

		Superimposition		Measurements	
		3D Slicer	Dolphin	3D Slicer	Dolphin
Examiner 1	Mean	13 min 60 sec	6 min 25 sec	6 min 49 sec	6 min 25 sec
	SD	2 min 30 sec	1 min 22 sec	1 min 50 sec	1 min 34 sec
	P-value	0.03 ^a		0.87	
Examiner 2	Mean	10 min 19 sec	5 min, 55 sec	12 min 25 sec	8 min 33 sec
	SD	1 min 59 sec	1 min 59 sec	2 min 58 sec	3 min 15 sec
	P-value	0.22		0.22	
Examiner 3	Mean	10 min 3 sec	4 min 15 sec	10 min 59 sec	7 min 9 sec
	SD	2 min 48 sec	1 min 2 sec	3 min 59 sec	1 min 55 sec
	P-value	0.036 ^a		0.215	
Overall	P-value	0.002 ^a		0.04 ^a	

^aStatistically significant at level $P < 0.05$ (paired t-test).

measurements between examiners and software ($P > 0.05$) (Tables 2 and 3). There was a significant difference in the SIP ($P < 0.05$), showing a mean increased time of 6.29 (SD 1 min) for 3D Slicer when compared to Dolphin Imaging (Table 1). This result may be associated with the manual superimposition used when evaluating two volumes in 3D Slicer, Dolphin Imaging, in turn, offers a voxel-based superior-imposition (automated) that allows for reduced time during this step of the analysis. Moreover, regarding the inter-examiner overall agreement for 3D Slicer measurements, all variables exhibited good agreement ($ICC \geq 0.8$) (Table 2); showing that either software can effectively provide reliable and reproducible linear measurements of bone dimensions adjacent to implants. When analysing buccal and lingual bone plates separately in both software, the palatal/lingual plates showed excellent agreement, with ICC values greater than 0.9, while the buccal bone thickness had lower agreement, with ICC values above 0.8 (Tables 2 and 3). The results of this study suggest that most changes in bone volume are associated with the buccal plate. Therefore, changes in bone density, height, and volume may have been inferred from these measurements.

Inter-examiner reliability
3D Slicer measurements

Inter-examiner agreement for 3D Slicer measurements showed good consistency ($ICC \geq 0.8$, F-test $P < 0.001$) across all variables for both BL (baseline) and T1 (follow-up). At BL and T1, implant width had an ICC of 0.802 (95% CI = 0.515 to 0.931), and implant height had an ICC of 0.93 (95% CI = 0.823 to 0.977) F-test with true value $P < 0.001$ (Table 2). For buccal bone thickness at different distances from the implant

shoulder in the sagittal view, ICC values were 0.813 to 0.884 at 0, 1, 3, and 5 mm. For lingual/palatal bone thickness, ICC values were 0.919 to 0.954 at 0, 1, 3, and 5 mm. At T1, implant width showed $ICC = 0.802$ (95% CI = 0.515 to 0.931), while reliability statistics with Cronbach’s α for single measurements showed $ICC = 0.93$ (95% CI = 0.823 to 0.977). Buccal bone thickness at T1 had ICC values of 0.801 to 0.943 at 0, 1, 3, and 5 mm. Lingual/palatal bone thickness at T1 had ICC values of 0.814 to 0.967 at 0, 1, 3, and 5 mm (Table 2).

Dolphin Imaging measurements

Dolphin Imaging measurements showed excellent agreement across variables at both BL and T1, with ICC values ranging from 0.806 to 0.961 (95% CI = 0.422 to 0.986), F-test $P < 0.001$. At BL and T1, implant height had $ICC = 0.898$ (95% CI = 0.75 to 0.965), and implant width at BL had $ICC = 0.8$ (95% CI = 0.528 to 0.933). For buccal bone thickness in the sagittal view, ICC values were 0.832 to 0.910 at 0, 1, 3, and 5 mm. For lingual/palatal bone thickness, ICC values were 0.893 to 0.958 at 0, 1, 3, and 5 mm. At T1, implant width showed a low $ICC = 0.537$ (95% CI = -0.441 to 0.851), indicating poor consistency. Reliability statistics showed Cronbach’s $\alpha = 0.93$, with ICC for single measurements at 0.814 (95% CI = 0.422 to 0.94), F-test $P < 0.001$. For buccal bone thickness at T1, ICC values were 0.806 to 0.961 at 0, 1, 3, and 5 mm. For lingual/palatal bone thickness, ICC values were 0.925 to 0.961 at all levels (Table 2).

Intra-examiner reliability
3D Slicer measurements

For 3D Slicer measurements, 5 out of 10 variables

Table 2. Intra-class coefficient (ICC) with 95% confidence intervals (CI) of inter-examiner 3D Slicer and Dolphin

Measurements		3D Slicer		Dolphin	
		Baseline (BL)	Follow-up (T1)	Baseline (BL)	Follow-up (T1)
		ICC (95% CI)	ICC (95% CI)	ICC (95% CI)	ICC (95% CI)
Buccal bone thickness	At 0 mm	0.835 (0.597; 0.943) ^a	0.801 (0.613; 0.931) ^a	0.908 (0.775; 0.968) ^a	0.806 (0.525; 0.933) ^a
	At 1 mm	0.884 (0.715; 0.96) ^a	0.943 (0.859; 0.98) ^a	0.91 (0.779; 0.969) ^a	0.961 (0.903; 0.986) ^a
	At 3 mm	0.869 (0.679; 0.954) ^a	0.894 (0.741; 0.963) ^a	0.866 (0.671; 0.953) ^a	0.905 (0.767; 0.967) ^a
	At 5 mm	0.813 (0.641; 0.935) ^a	0.815 (0.647; 0.936) ^a	0.832 (0.689; 0.942) ^a	0.874 (0.69; 0.956) ^a
Palatal bone thickness	At 0 mm	0.919 (0.802; 0.972) ^a	0.814 (0.643; 0.935) ^a	0.893 (0.738; 0.963) ^a	0.925 (0.816; 0.974) ^a
	At 1 mm	0.954 (0.887; 0.984) ^a	0.967 (0.918; 0.988) ^a	0.948 (0.872; 0.982) ^a	0.961 (0.905; 0.986) ^a
	At 3 mm	0.925 (0.817; 0.974) ^a	0.92 (0.805; 0.972) ^a	0.958 (0.898; 0.985) ^a	0.944 (0.863; 0.981) ^a
	At 5 mm	0.929 (0.825; 0.975) ^a	0.887 (0.722; 0.961) ^a	0.897 (0.749; 0.964) ^a	0.932 (0.833; 0.976) ^a
Implant	Width	0.802 (0.515; 0.931) ^a	0.802 (0.515; 0.931) ^a	0.808 (0.528; 0.933) ^a	0.537 (0.422; 0.986)
	Height	0.93 (0.823; 0.977) ^a	0.93 (0.823; 0.977) ^a	0.898 (0.75; 0.965) ^a	0.898 (0.75; 0.986) ^a

^aF-test with true value P < 0.001 and reliability statistics with Cronbach's α, for single measurements > 0.90.

Table 3. Intra-class coefficient (ICC) with 95% confidence intervals (CI) of intra-examiner 3D Slicer and Dolphin

Measurements		3D Slicer		Dolphin	
		Baseline (BL)	Follow-up (T1)	Baseline (BL)	Follow-up (T1)
		ICC (95% CI)	ICC (95% CI)	ICC (95% CI)	ICC (95% CI)
Buccal bone thickness	At 0 mm	0.734 (0.6; -0.915)	0.949 (0.841; 0.984) ^a	0.936 (0.801; 0.979) ^a	0.908 (0.713; 0.97) ^a
	At 1 mm	0.824 (0.451; 0.943) ^a	0.56 (0.5; 0.734)	0.967 (0.898; 0.99) ^a	0.952 (0.851; 0.985) ^a
	At 3 mm	0.817 (0.429; 0.941) ^a	0.606 (-0.226; -0.874)	0.967 (0.898; 0.989) ^a	0.967 (0.898; 0.989) ^a
	At 5 mm	0.786 (0.333; 0.931) ^a	0.787 (0.338; 0.932) ^a	0.993 (0.977; 0.998) ^a	0.993 (0.977; 0.998) ^a
Palatal bone thickness	At 0 mm	0.619 (-1.933; 0.698)	0.903 (0.698; 0.969) ^a	0.959 (0.872; 0.987) ^a	0.959 (0.872; -0.987) ^a
	At 1 mm	0.854 (-0.87; 0.999) ^a	0.895 (0.672; 0.966) ^a	0.975 (0.922; 0.992) ^a	0.984 (0.922; 0.997) ^a
	At 3 mm	0.725 (-0.778; 0.817)	0.633 (-0.142; 0.882)	0.977 (0.929; 0.993) ^a	0.978 (0.929; 0.993) ^a
	At 5 mm	0.929 (0.679; 0.997)	0.738 (-0.07; -0.89)	0.886 (0.645; 0.963) ^a	0.963 (0.845; 0.963) ^a
Implant	Width	0.956 (0.863; 0.986) ^a	0.949 (0.841; 0.984) ^a	0.933 (0.792; 0.979) ^a	0.824 (0.452; 0.943) ^a
	Height	0.999 (0.995; 1) ^a	0.997 (0.992; 0.999) ^a	0.992 (0.976; 0.997) ^a	0.992 (0.974; 0.997) ^a

^aF-test with true value P < 0.001 and reliability statistics with Cronbach's α, for single measurements > 0.90.

showed good agreement (ICC ≥ 0.8) between the first and second measurements at both BL and T1. Implant width had ICC = 0.956 (95% CI = 0.863 to 0.986) at BL and ICC = 0.949 (95% CI = 0.841 to 0.984) at T1, indicating excellent consistency. Implant height showed near-perfect agreement with ICC = 0.999 (95% CI = 0.995 to 1.000) at BL and ICC = 0.997 (95% CI = 0.992 to 0.999) at T1 (Table 3). In the sagittal view buccal at BL, measurements at 1, 3, and 5 mm showed moderate to good agreement (0.78 < ICC < 0.85): ICC = 0.824 (95% CI = 0.451 to 0.943). At T1, only the 3 mm buccal measurement showed moderate agreement (ICC = 0.787, 95% CI = 0.338 to 0.932). The sagittal view lingual/palatal at T1 showed good agreement for both 0 and 1 mm measurements: ICC > 0.903 (95% CI = 0.698 to 0.969) at 0, and 1 mm (Table 3).

Dolphin Imaging measurements

For the Dolphin Imaging measurements, all variables demonstrated good agreement (ICC ≥ 0.8) between measurements on BL and T1 (0.824 to 0.992), with 95% CI ranging from moderate to excellent (0.452 to 0.997) (Table 3).

DISCUSSION

The critical role of peri-implant bone volume and soft tissue seems to be of importance [27,28]. Previous studies have evaluated the accuracy of CBCT [23,29]. However, there are limited reports on CBCT, concerning intra-examiner and inter-examiner evaluations [30,31]. Song et al. [32] studied the accuracy of CBCT versus radiography in detecting,

classifying, and measuring peri-implant bone defects in an animal model. The study used 54 mandible blocks from beagle dogs. Images were obtained with IO, CBCT, and micro-CT. Defects were diagnosed and classified as either dehiscence, infrabony, or crater-like. Observers evaluated defect location, shape, depth, and width using IO and CBCT images. CBCT demonstrated higher diagnostic accuracy (100% sensitivity) compared to IO (69% sensitivity), and was superior in defect classification and measurement, closely correlating with the gold standard micro-CT. CBCT offers significant diagnostic and decision-making advantages over conventional IO imaging for peri-implant bone defects. Nonetheless, it is important to highlight the limitations of CBCT such as image artifacts from nearby radio-dense (metallic) objects that can affect diagnostic evaluations. For example, a thin buccal bone (< 0.5 mm) or a buccal bone adjacent to metallic structures, like implants, can produce artifacts that severely degrade image quality and, as a result, compromise diagnostic precision [8]. This could partially explain the results in measuring the buccal plate changes in the present study.

A previous study used dry human skulls to measure the alveolar bone height using the cemento-enamel junction as a reference [33]. Findings showed an accuracy of 0.6 mm and 0.4 mm, respectively when compared to clinical measurements using a caliper. One study showed a moderate correlation between CBCT and ridge mapping in edentulous human ridges (R-squared: 0.53 and 94.6% correlation of measurements within a 95% confidence interval) with reported overall ICC values of 0.61 to 0.93 and 0.4 to 0.95 for two observers [15]. In addition, an *in vivo* study confirmed the accuracy of CBCT when measuring vertical bone defects on the mesial and distal surfaces of teeth; when compared to direct clinical measurements (gold standard), and intraoral radiographs [34]. Similarly, a high correlation between CBCT and direct clinical measurements in extraction sockets (buccolingual: 0.782 [P < 0.05], mesiodistal: 0.983 [P < 0.01]) was shown in an *in vivo* study [19]. A high ICC value was also reported by Sheikhi et al. [22] for height (ICC = 0.89) as well as width (ICC = 0.91). A total of 94.6% of the data for ridge mapping, CBCT, and clinical gold standard measurements were within the mean and one standard deviation in a Bland-Altman plot by Eachempati et al. [15]. Several authors have used CBCT images to report bone measurements that are considered accurate if the errors are less than 1 millimeter [29,35]. A clear trend of underestimation or overestimation was not evident. The mean measurement error (ME) in millimeters between two

values was assessed [22,29]. The mean difference between CBCT and direct clinical examination was 0.22 (SD 0.15) mm and a maximum error of 1 mm. The mean absolute percentage of error was 1.4% with a range of 0.1 to 5.2% [29]. Other studies reported range differences from 0.3 to 0.6 mm [36].

A systematic review by Fokas et al. [37] evaluated the accuracy of linear measurements using maxillofacial CBCT in implant dentistry. The review analysed 22 studies that focused on CBCT measurements of alveolar bone and anatomical distances relevant to implant placement. The findings indicated that CBCT provides highly accurate and reliable measurements, with a voxel size of 0.3 to 0.4 mm suitable for implant planning. Accuracy can be affected by factors such as patient motion, metallic artifacts, and software settings, underscoring the need for careful inter- and intra-examiner calibration. Another review by Lou et al. [38], assessed the accuracy and reliability of landmark identification using CT and CBCT in the maxillofacial. The study analysed eight articles, noting that different landmarks exhibited varying degrees of ME. The review emphasized that with repeated practice, the error for 2D CT could be reduced to within 0.5 mm, though some 3D CT reliability values still require careful consideration due to their potential diagnostic implications.

Additionally, 3D Slicer, an open-source software is useful for visualizing medical data and analysing images for clinical research [24,39]. Recently, investigators in medical and engineering research have concentrated on developing 3D Slicer modules and algorithms that enable users to manage datasets from various organs and integrate multi-modal images. These include magnetic resonance imaging (MRI), computed tomography (CT), CBCT, ultrasound (US), nuclear medicine, and microscopy [39,40]. Advances in periodontics have incorporated the use of multiple volumes such as CBCT, IO, and ultrasound images of teeth, implants, and edentulous crests [41]. This study developed and validated a method for accurately registering US images of the jawbone, improving the precision of US imaging compared to freehand scans using 3D Slicer to register and analyse the accuracy of the superimposed modalities. A validation study and a registration method demonstrated superior repeatability and accuracy, particularly in mapping both soft and hard tissues of the edentulous ridge, when compared to CBCT, IO and the use of 3D Slicer suggested that this method enhances the reliability of longitudinal evaluations of tissue changes [41]. The same study group [42] evaluated micro-CT measurements of

bone mineral density and bone volume fraction using the “bone texture extension” of 3D Slicer [42]. Other applications in dentistry include the use of craniomaxillofacial modules that feature user-friendly algorithms for minimally invasive diagnostics through multimodal image integration and analysis. These modules offer a comprehensive approach to managing data extraction, registration, visualization, and quantification from various sources [43]. Tools like patient-specific 3D mesh models and label map creation enhance clinicians’ ability to make informed decisions, perform data analysis, and visualize personalized healthcare solutions.

Dolphin Imaging can be used for 3D superimpositions using open-source and commercial software versions [25]. It is a commercially available tool, offers a significant advantage in terms of convenience, speed, and user-friendly voxel-based superimposition method that completes the process in under five minutes. This significant advantage over other open-source alternatives that took about three hours [25]. Dolphin Imaging 3D has been widely used in orthodontics [44,45]. Studies vary from investigating the position of alveolar cortex in response to tooth movement in extraction and non-extraction cases using CBCT [46]. to digital workflow for combined orthodontic movement and orthognathic surgery approach [44], and in the comparison of effectiveness and validity of two systems for surgical planning in dentofacial deformities [45]. In clinical orthodontics, the accurate and efficient superimposition of CBCT images is crucial for evaluating craniofacial growth and treatment effects [25]. There are three primary methods for superimposing 3D images: landmark-based, surface-based, and voxel-based. Landmark-based superimposition uses anatomical landmarks but is more complex in 3D due to the difficulty of identifying landmarks compared to 2D radiographs. Surface-based superimposition relies on high-quality 3D surface models and is effective in quantifying midfacial changes. Voxel-based superimposition [47], uses voxel density matching for automated, accurate superimposition, thus reducing operator error.

High reproducibility and repeatability of measurements are essential in evaluating the consistency of measurements between observers and follow-up patients longitudinally. The correlations between intra-examiner and inter-examiner proved to be a positive method in several studies of CBCT, as well as available software-made precise measurements performed by different professionals [48]. A previous study evaluated CBCT scans from 50 patients in which two examiners independently identified landmarks in both 2D and 3D images on

two separate occasions, with a one-week interval between sessions. Intra- and inter-examiner reproducibility and reliability were assessed. The analysis demonstrated high examiner reproducibility for both linear and volumetric parameters, with high ICC and low CV, indicating that the methodology is highly reliable and reproducible [48]. A human cadaver mandible was examined in two edentulous areas and one dentate area using both dry and sucrose-immersed CBCT and multislice conventional tomography (MSCT) to assess the accuracy of linear measurements [23]. Two readers measured four linear distances twice from each section. The mandible was cut into 4 mm slices at three marked places and micro-radiographed. Intraclass correlations for intra- and inter-observer readings were almost perfect (ICC = 1). ME significantly differed between methods (P = 0.022). The mean ME was 4.7% for dry CBCT, 8.8% for dry MSCT, 2.3% for sucrose CBCT, and 6.6% for sucrose MSCT. Findings indicate that CBCT is a reliable tool for implant-planning measurements. Significant radiation dose reduction is achievable with low-dose MSCT without major significant loss of measurement accuracy [23]. Additionally, the level of experience with CBCT images and software may have significantly impacted inter-examiner reliability [30]. According to Lagravere et al. [30], variations in landmark identification greater than 1.0 mm are considered clinically significant. The clinical relevance of such variations also depends on the size of the structure being assessed and the magnitude of the change being measured. In this study, some measurements, particularly those assessed by different examiners, exhibited variations exceeding this threshold.

Successful implant treatment outcomes should incorporate a detailed planning phase with images of diagnostic quality. Assessing bone quantity and quality and identifying vital structures will maximize the long-term success of implants [49]. A voxel size of 0.3 to 0.4 mm is ideal for CBCT imaging data of acceptable diagnostic quality. Implant survival rates have shown to be higher in cases of partial and full edentulism for implants and their restorations [50]. The encouraging clinical results of implants have led to increased implant indications in partially edentulous individuals for rehabilitation [50]. Long-term outcomes seem to be a concern for clinicians due to biological, prosthetic, and esthetical complications [49].

CONCLUSIONS

To conclude, the study found that while 3D Slicer

offered superior image quality, Dolphin Imaging excelled in voxel-based superimposition. Both methods demonstrated high examiner reproducibility for linear and volumetric measurements, with intraclass correlation coefficients above 0.8 and low coefficients of variation, highlighting their reliability and consistency. Specifically, 3D Slicer achieved excellent overall inter-examiner agreement for all variables (intraclass correlation coefficient ≥ 0.80), with no significant differences compared to Dolphin Imaging. Variations in results were attributed to differences in landmark interpretation, individual anatomical variations, and examiner experience with cone-beam computed tomography images and software, aligning with findings from other studies. The measurements showed strong agreement between examiners (intraclass correlation coefficient > 0.80), with significant reliability and reproducibility. This methodology is well-suited as a standard for precise linear measurement analysis of osseous structures around implants. With careful landmark selection and appropriate measurement tools, this approach can provide clear and accurate information essential for precise diagnosis.

ACKNOWLEDGMENTS AND DISCLOSURE STATEMENTS

Declaration of interest: none

Funding statement: this research received no specific grant from any funding agency in the public, commercial, or not-for-profit sectors.

Acknowledgements: we acknowledge the University of Illinois Chicago School of Dentistry, Periodontics Department, for their support in providing facilities and software resources.

Authors contributions: Amanda B. Rodriguez, and Tolga Fikret Tozum have contributed substantially to the study's conception and design. Amanda B. Rodriguez, Berceste Guler Ayyildiz, Halil Ayyildiz, Aniruddh Narvekar, and Grace Viana have been involved in data collection and data analysis. Amanda B. Rodriguez, Berceste Guler Ayyildiz, Halil Ayyildiz, Aniruddh Narvekar, Mohammed H. Elnagar, Michael Schmerman, Salvador Nares, and Tolga Tozum have been involved in data interpretation, drafting the manuscript, and revising it critically and have given final approval of the version to be published.

REFERENCES

1. Monje A, Pons R, Rocuzzo A, Salvi GE, Nart J. Reconstructive therapy for the management of peri-implantitis via submerged guided bone regeneration: A prospective case series. *Clin Implant Dent Relat Res*. 2020 Jun;22(3):342-350. [Medline: [32410379](#)] [doi: [10.1111/cid.12913](#)]
2. Sinjab K, Garaicoa-Pazmino C, Wang HL. Decision Making for Management of Periimplant Diseases. *Implant Dent*. 2018 Jun;27(3):276-281. [Medline: [29762186](#)] [doi: [10.1097/ID.0000000000000775](#)]
3. Derks J, Tomasi C. Peri-implant health and disease. A systematic review of current epidemiology. *J Clin Periodontol*. 2015 Apr;42 Suppl 16:S158-71. [Medline: [12787220](#)] [doi: [10.1111/jcpe.12334](#)]
4. Berglundh T, Persson L, Klinge B. A systematic review of the incidence of biological and technical complications in implant dentistry reported in prospective longitudinal studies of at least 5 years. *J Clin Periodontol*. 2002;29 Suppl 3: 197-212; discussion 232-3. [Medline: [12787220](#)] [doi: [10.1034/j.1600-051X.29.s3.12.x](#)]
5. Chan HL, Benavides E, Yeh CY, Fu JH, Rudek IE, Wang HL. Risk assessment of lingual plate perforation in posterior mandibular region: a virtual implant placement study using cone-beam computed tomography. *J Periodontol*. 2011 Jan;82(1):129-35. [Medline: [20653440](#)] [doi: [10.1902/jop.2010.100313](#)]
6. Berglundh T, Jepsen S, Stadlinger B, Terheyden H. Peri-implantitis and its prevention. *Clin Oral Implants Res*. 2019 Feb;30(2):150-155. [Medline: [30636066](#)] [doi: [10.1111/clr.13401](#)]
7. Ko TJ, Byrd KM, Kim SA. The Chairside Periodontal Diagnostic Toolkit: Past, Present, and Future. *Diagnostics (Basel)*. 2021 May 22;11(6):932. [Medline: [34067332](#)] [PMC free article: [8224643](#)] [doi: [10.3390/diagnostics11060932](#)]
8. Rodriguez Betancourt A, Samal A, Chan HL, Kripfgans OD. Overview of Ultrasound in Dentistry for Advancing Research Methodology and Patient Care Quality with Emphasis on Periodontal/Peri-implant Applications. *Z Med Phys*. 2023 Aug;33(3):336-386. [Medline: [36922293](#)] [PMC free article: [10517409](#)] [doi: [10.1016/j.zemedi.2023.01.005](#)]
9. Hilgenfeld T, Juerchott A, Deisenhofer UK, Krisam J, Rammelsberg P, Heiland S, Bendszus M, Schwindling FS. Accuracy of cone-beam computed tomography, dental magnetic resonance imaging, and intraoral radiography for detecting peri-implant bone defects at single zirconia implants-An in vitro study. *Clin Oral Implants Res*. 2018 Sep;29(9):922-930. [Medline: [30112833](#)] [doi: [10.1111/clr.13348](#)]
10. Abdinian M, Aminian M, Seyyedkhamesi S. Comparison of accuracy between panoramic radiography, cone-beam computed tomography, and ultrasonography in detection of foreign bodies in the maxillofacial region: an in vitro study. *J Korean Assoc Oral Maxillofac Surg*. 2018 Feb;44(1):18-24. [Medline: [29535965](#)] [PMC free article: [5845963](#)] [doi: [10.5125/jkaoms.2018.44.1.18](#)]

11. Suomalainen A, Kiljunen T, Käser Y, Peltola J, Kortnesniemi M. Dosimetry and image quality of four dental cone beam computed tomography scanners compared with multislice computed tomography scanners. *Dentomaxillofac Radiol*. 2009 Sep;38(6):367-78. [Medline: [19700530](#)] [doi: [10.1259/dmfr/15779208](#)]
12. Nguyen KT, Pachêco-Pereira C, Kaipatur NR, Cheung J, Major PW, Le LH. Comparison of ultrasound imaging and cone-beam computed tomography for examination of the alveolar bone level: A systematic review. *PLoS One*. 2018 Oct 3;13(10):e0200596. [Medline: [30281591](#)] [PMC free article: [6169851](#)] [doi: [10.1371/journal.pone.0200596](#)]
13. Fokas G, Vaughn VM, Scarfe WC, Bornstein MM. Accuracy of linear measurements on CBCT images related to presurgical implant treatment planning: A systematic review. *Clin Oral Implants Res*. 2018 Oct;29 Suppl 16:393-415. [Medline: [30328204](#)] [doi: [10.1111/clr.13142](#)]
14. Woelber JP, Fleiner J, Rau J, Ratka-Krüger P, Hannig C. Accuracy and Usefulness of CBCT in Periodontology: A Systematic Review of the Literature. *Int J Periodontics Restorative Dent*. 2018 Mar/Apr;38(2):289-297. [Medline: [29447324](#)] [doi: [10.11607/prd.2751](#)]
15. Eachempati P, Vynne OJ, Annishka A, Fickry FSS, Naurah MA, Idiculla JJ, Soe HHK. A comparative cross-sectional study of pre-implant site assessment using ridge mapping and orthopantomography (OPG) with cone beam computed tomography (CBCT). *RJPBCS*. 2016 Sep-Oct;7(5):1185-92. [URL: [https://www.rjpbcs.com/pdf/2016_7\(5\)/\[146\].pdf](https://www.rjpbcs.com/pdf/2016_7(5)/[146].pdf)]
16. Freire-Maia B, Machado VD, Valerio CS, Custódio AL, Manzi FR, Junqueira JL. Evaluation of the accuracy of linear measurements on multi-slice and cone beam computed tomography scans to detect the mandibular canal during bilateral sagittal split osteotomy of the mandible. *Int J Oral Maxillofac Surg*. 2017 Mar;46(3):296-302. [Medline: [27939592](#)] [doi: [10.1016/j.ijom.2016.11.007](#)]
17. Ganguly R, Ramesh A, Pagni S. The accuracy of linear measurements of maxillary and mandibular edentulous sites in cone-beam computed tomography images with different fields of view and voxel sizes under simulated clinical conditions. *Imaging Sci Dent*. 2016 Jun;46(2):93-101. [Medline: [27358816](#)] [PMC free article: [4925656](#)] [doi: [10.5624/isd.2016.46.2.93](#)]
18. Al-Ekrish AA, Ekram MI, Al Faleh W, Alkhader M, Al-Sadhan R. The validity of different display monitors in the assessment of dental implant site dimensions in cone beam computed tomography images. *Acta Odontol Scand*. 2013 Sep;71(5):1085-91. [Medline: [23167840](#)] [doi: [10.3109/00016357.2012.741709](#)]
19. Alkan BA, Aral CA, Aral K, Acer N, Şişman Y. Quantification of circumferential bone level and extraction socket dimensions using different imaging and estimation methods: a comparative study. *Oral Radiol*. 2016 Sep;32:145-53. [doi: [10.1007/s11282-015-0225-5](#)]
20. Luk LC, Pow EH, Li TK, Chow TW. Comparison of ridge mapping and cone beam computed tomography for planning dental implant therapy. *Int J Oral Maxillofac Implants*. 2011 Jan-Feb;26(1):70-4. [Medline: [21365040](#)]
21. Luangchana P, Pornprasertsuk-Damrongsri S, Kiattavorncharoen S, Jirajariyavej B. Accuracy of linear measurements using cone beam computed tomography and panoramic radiography in dental implant treatment planning. *Int J Oral Maxillofac Implants*. 2015 Nov-Dec;30(6):1287-94. [Medline: [26574854](#)] [doi: [10.11607/jomi.4073](#)]
22. Sheikhi M, Dakhil-Alian M, Bahreinian Z. Accuracy and reliability of linear measurements using tangential projection and cone beam computed tomography. *Dent Res J (Isfahan)*. 2015 May-Jun;12(3):271-7. [Medline: [26005469](#)] [PMC free article: [4432612](#)]
23. Suomalainen A, Vehmas T, Kortnesniemi M, Robinson S, Peltola J. Accuracy of linear measurements using dental cone beam and conventional multislice computed tomography. *Dentomaxillofac Radiol*. 2008 Jan;37(1):10-7. [Medline: [18195249](#)] [doi: [10.1259/dmfr/14140281](#)]
24. Fedorov A, Beichel R, Kalpathy-Cramer J, Finet J, Fillion-Robin JC, Pujol S, Bauer C, Jennings D, Fennessy F, Sonka M, Buatti J, Aylward S, Miller JV, Pieper S, Kikinis R. 3D Slicer as an image computing platform for the Quantitative Imaging Network. *Magn Reson Imaging*. 2012 Nov;30(9):1323-41. [Medline: [22770690](#)] [PMC free article: [3466397](#)] [doi: [10.1016/j.mri.2012.05.001](#)]
25. Bazina M, Cevidanes L, Ruellas A, Valiathan M, Qureshy F, Syed A, Wu R, Palomo JM. Precision and reliability of Dolphin 3-dimensional voxel-based superimposition. *Am J Orthod Dentofacial Orthop*. 2018 Apr;153(4):599-606. [Medline: [29602352](#)] [doi: [10.1016/j.ajodo.2017.07.025](#)]
26. Park CH, Abramson ZR, Taba M Jr, Jin Q, Chang J, Kreider JM, Goldstein SA, Giannobile WV. Three-dimensional micro-computed tomographic imaging of alveolar bone in experimental bone loss or repair. *J Periodontol*. 2007 Feb;78(2):273-81. [Medline: [17274716](#)] [PMC free article: [2581750](#)] [doi: [10.1902/jop.2007.060252](#)]
27. Giannobile WV, Jung RE, Schwarz F; Groups of the 2nd Osteology Foundation Consensus Meeting. Evidence-based knowledge on the aesthetics and maintenance of peri-implant soft tissues: Osteology Foundation Consensus Report Part 1-Effects of soft tissue augmentation procedures on the maintenance of peri-implant soft tissue health. *Clin Oral Implants Res*. 2018 Mar;29 Suppl 15:7-10. [Medline: [29498127](#)] [doi: [10.1111/clr.13110](#)]
28. Thoma DS, Naenni N, Figuero E, Hämmerle CHF, Schwarz F, Jung RE, Sanz-Sánchez I. Effects of soft tissue augmentation procedures on peri-implant health or disease: A systematic review and meta-analysis. *Clin Oral Implants Res*. 2018 Mar;29 Suppl 15:32-49. [Medline: [29498129](#)] [doi: [10.1111/clr.13114](#)]
29. Kobayashi K, Shimoda S, Nakagawa Y, Yamamoto A. Accuracy in measurement of distance using limited cone-beam computerized tomography. *Int J Oral Maxillofac Implants*. 2004 Mar-Apr;19(2):228-31. [Medline: [15101594](#)]

30. Lagravère MO, Gordon JM, Guedes IH, Flores-Mir C, Carey JP, Heo G, Major PW. Reliability of traditional cephalometric landmarks as seen in three-dimensional analysis in maxillary expansion treatments. *Angle Orthod.* 2009 Nov;79(6):1047-56. [Medline: [19852593](#)] [doi: [10.2319/010509-10R.1](#)]
31. Ludlow JB, Laster WS, See M, Bailey LJ, Hershey HG. Accuracy of measurements of mandibular anatomy in cone beam computed tomography images. *Oral Surg Oral Med Oral Pathol Oral Radiol Endod.* 2007 Apr;103(4):534-42. [Medline: [17395068](#)] [PMC free article: [3644804](#)] [doi: [10.1016/j.tripleo.2006.04.008](#)]
32. Song D, Shujaat S, de Faria Vasconcelos K, Huang Y, Politis C, Lambrechts I, Jacobs R. Diagnostic accuracy of CBCT versus intraoral imaging for assessment of peri-implant bone defects. *BMC Med Imaging.* 2021 Feb 10;21(1):23. [Medline: [33568085](#)] [PMC free article: [7877020](#)] [doi: [10.1186/s12880-021-00557-9](#)]
33. Leung CC, Palomo L, Griffith R, Hans MG. Accuracy and reliability of cone-beam computed tomography for measuring alveolar bone height and detecting bony dehiscences and fenestrations. *Am J Orthod Dentofacial Orthop.* 2010 Apr;137(4 Suppl):S109-19. [Medline: [20381751](#)] [doi: [10.1016/j.ajodo.2009.07.013](#)]
34. Grimard BA, Hoidal MJ, Mills MP, Mellonig JT, Nummikoski PV, Mealey BL. Comparison of clinical, periapical radiograph, and cone-beam volume tomography measurement techniques for assessing bone level changes following regenerative periodontal therapy. *J Periodontol.* 2009 Jan;80(1):48-55. [Medline: [19228089](#)] [doi: [10.1902/jop.2009.080289](#)]
35. Torres MG, Campos PS, Segundo NP, Navarro M, Crusoé-Rebello I. Accuracy of linear measurements in cone beam computed tomography with different voxel sizes. *Implant Dent.* 2012 Apr;21(2):150-5. [Medline: [22382754](#)] [doi: [10.1097/ID.0b013e31824bf93c](#)]
36. Veyre-Goulet S, Fortin T, Thierry A. Accuracy of linear measurement provided by cone beam computed tomography to assess bone quantity in the posterior maxilla: a human cadaver study. *Clin Implant Dent Relat Res.* 2008 Dec;10(4):226-30. [Medline: [18384410](#)] [doi: [10.1111/j.1708-8208.2008.00083.x](#)]
37. Fokas G, Vaughn VM, Scarfe WC, Bornstein MM. Accuracy of linear measurements on CBCT images related to presurgical implant treatment planning: A systematic review. *Clin Oral Implants Res.* 2018 Oct;29 Suppl 16:393-415. [Medline: [30328204](#)] [doi: [10.1111/clr.13142](#)]
38. Lou L, Lagravere MO, Compton S, Major PW, Flores-Mir C. Accuracy of measurements and reliability of landmark identification with computed tomography (CT) techniques in the maxillofacial area: a systematic review. *Oral Surg Oral Med Oral Pathol Oral Radiol Endod.* 2007 Sep;104(3):402-11. [Medline: [17709072](#)] [doi: [10.1016/j.tripleo.2006.07.015](#)]
39. Pieper S, Halle M, Kikinis R. "3D Slicer". In: *Proceedings of the 2004 2nd IEEE International Symposium on Biomedical Imaging: Nano to Macro (IEEE Cat No. 04EX821)*; Arlington, VA, USA. 15-18 April 2004. p. 632-5. Vol. 1. [doi: [10.1109/ISBI.2004.1398617](#)]
40. S. Pieper, M. Halle and R. Kikinis, "3D Slicer," 2004 2nd IEEE International Symposium on Biomedical Imaging: Nano to Macro (IEEE Cat No. 04EX821). Arlington, VA, USA. 2004; Vol. 1. p. 632-5. [doi: [10.1109/ISBI.2004.1398617](#)]
41. Rodriguez Betancourt A, Kripfgans OD, Meneghetti PC, Mendonça G, Pereira R, Teixeira W, Zambrana N, Samal A, Chan HL. Intraoral ultrasonography image registration for evaluation of partial edentulous ridge: A methodology and validation study. *J Dent.* 2024 Sep;148:105136. [Medline: [38885734](#)] [doi: [10.1016/j.jdent.2024.105136](#)]
42. Rodriguez AB, Kripfgans OD, Kozloff KM, Samal A, Woo JM, Shehabeldin M, Chan HL. Ultrasound-based jawbone surface quality evaluation after alveolar ridge preservation. *J Periodontol.* 2024 Dec;95(12):1150-1159. [Medline: [38742564](#)] [PMC free article: [11708450](#)] [doi: [10.1002/JPER.23-0370](#)]
43. Bianchi J, Paniagua B, De Oliveira Ruellas AC, Fillion-Robin JC, Prietro JC, Gonçalves JR, Hctor J, Yatabe M, Styner M, Li T, Gurgel ML, Chaves CM, Massaro C, Garib DG, Vilanova L, Castanha Henriques JF, Aliaga-Del Castillo A, Janson G, Iwasaki LR, Nickel JC, Evangelista K, Cevidanes L. 3D Slicer Craniomaxillofacial Modules Support Patient-Specific Decision-Making for Personalized Healthcare in Dental Research. *Multimodal Learn Clin Decis Support Clin Image Based Proc (2020)*. 2020 Oct;12445:44-53. [Medline: [33415323](#)] [PMC free article: [7786614](#)] [doi: [10.1007/978-3-030-60946-7_5](#)]
44. Elnagar MH, Aronovich S, Kusnoto B. Digital Workflow for Combined Orthodontics and Orthognathic Surgery. *Oral Maxillofac Surg Clin North Am.* 2020 Feb;32(1):1-14. [Medline: [31699582](#)] [doi: [10.1016/j.coms.2019.08.004](#)]
45. Piombino P, Abbate V, Sani L, Troise S, Committeri U, Carraturo E, Maglito F, De Riu G, Vaira LA, Califano L. Virtual Surgical Planning in Orthognathic Surgery: Two Software Platforms Compared. *Appl. Sci.* 2022 Sep; 12(18):9364. [doi: [10.3390/app12189364](#)]
46. Yang CYM, Atsawasuwan P, Viana G, Tozum TF, Elshebiny T, Palomo JM, Sellke T, Elnagar MH. Cone-beam computed tomography assessment of maxillary anterior alveolar bone remodelling in extraction and non-extraction orthodontic cases using stable extra-alveolar reference. *Orthod Craniofac Res.* 2023 May;26(2):265-276. [Medline: [36104955](#)] [doi: [10.1111/ocr.12609](#)]
47. Cevidanes LH, Bailey LJ, Tucker GR Jr, Styner MA, Mol A, Phillips CL, Proffit WR, Turvey T. Superimposition of 3D cone-beam CT models of orthognathic surgery patients. *Dentomaxillofac Radiol.* 2005 Nov;34(6):369-75. [Medline: [16227481](#)] [PMC free article: [3552302](#)] [doi: [10.1259/dmfr/17102411](#)]
48. Santos Tde S, Gomes AC, de Melo DG, Melo AR, Cavalcante JR, de Araújo LC, Travassos RM, Martins-Filho PR, Piva MR, Silva HF. Evaluation of reliability and reproducibility of linear measurements of cone-beam-computed tomography. *Indian J Dent Res.* 2012 Jul-Aug;23(4):473-8. [Medline: [23257480](#)] [doi: [10.4103/0970-9290.104952](#)]

49. Zucchelli G, Tavelli L, Stefanini M, Barootchi S, Mazzotti C, Gori G, Wang HL. Classification of facial peri-implant soft tissue dehiscence/deficiencies at single implant sites in the esthetic zone. *J Periodontol*. 2019 Oct;90(10):1116-1124. [Medline: [31087334](#)] [doi: [10.1002/JPER.18-0616](#)]
50. Pjetursson BE, Thoma D, Jung R, Zwahlen M, Zembic A. A systematic review of the survival and complication rates of implant-supported fixed dental prostheses (FDPs) after a mean observation period of at least 5 years. *Clin Oral Implants Res*. 2012 Oct;23 Suppl 6:22-38. [Medline: [23062125](#)] [doi: [10.1111/j.1600-0501.2012.02546.x](#)]

To cite this article:

Rodriguez AB, Ayyildiz BG, Ayyildiz H, Narvekar A, Elnagar MH, Schmerman M, Viana G, Nares S, Tözüm TF. CBCT Validation Study on Intraclass Correlation for Linear Measurements in Peri-implantitis: an Observational Study *J Oral Maxillofac Res* 2025;16(1):e4
URL: <http://www.ejomr.org/JOMR/archives/2025/1/e4/v16n1e4.pdf>
doi: [10.5037/jomr.2025.16104](#)

Copyright © Rodriguez AB, Ayyildiz BG, Ayyildiz H, Narvekar A, Elnagar MH, Schmerman M, Viana G, Nares S, Tözüm TF. Published in the JOURNAL OF ORAL & MAXILLOFACIAL RESEARCH (<http://www.ejomr.org>), 31 March 2025. This is an open-access article, first published in the JOURNAL OF ORAL & MAXILLOFACIAL RESEARCH, distributed under the terms of the [Creative Commons Attribution-Noncommercial-No Derivative Works 3.0 Unported License](#), which permits unrestricted non-commercial use, distribution, and reproduction in any medium, provided the original work and is properly cited. The copyright, license information and link to the original publication on (<http://www.ejomr.org>) must be included.